

Research report

C-terminal phosphorylation of the high molecular weight neurofilament subunit correlates with decreased neurofilament axonal transport velocity

Cheolwha Jung, Jason T. Yabe, Thomas B. Shea *

Department of Biological Sciences, Center for Cellular Neurobiology and Neurodegeneration Research, University of Massachusetts, Lowell One University Avenue, Lowell, MA, 01854 USA

Accepted 2 November 1999

Abstract

We probed the relationship of NF axonal transport of neurofilaments (NFs) to their phosphorylation state by comparing these parameters in two closely-aged groups of young adult mice — 2 and 5 months of age. This particular time interval was selected since prior studies demonstrate that optic axons have already completed axonal caliber expansion and attained adult NF levels by 2 months but, as shown herein, continue to increase NF-H C-terminal phosphorylation. NF axonal transport was monitored by autoradiographic analysis of the distribution of radiolabeled subunits immunoprecipitated from optic axon segments at intervals following intravitreal injection of ³⁵S-methionine. Both the peak and front of radiolabeled NFs translocated faster in 2- vs. 5-month-old mice. This developmental decline in NF transport rate was not due to reduced incorporation of NFs into the cytoskeleton, nor to an overall decline in slow axonal transport. By excluding or minimizing other factors, these findings support previous conclusions that C-terminal NF phosphorylation regulates NF axonal transport. © 2000 Published by Elsevier Science B.V. All rights reserved.

Keywords: Neurofilament; Axonal transport; Phosphorylation; Cytoskeleton; Axon; Development; Aging

1. Introduction

Like all constituents of the axonal cytoskeleton, neurofilaments (NFs) are synthesized within the neuronal perikaryon and are subsequently delivered to the axon by a process referred to as axonal transport [20,26]. The mode of NF axonal transport has not been determined, but, like other aspects of NF behavior, is thought to be regulated by phosphorylation [6,11,14,15,19,24,25,33,44]. Distinct kinases phosphorylate the N-terminal and C-terminal portion of NFs [14,27,28,31,37–39] and, in doing so, are thought to modulate aspects of NF assembly and interaction with other cytoskeletal proteins and their putative transport motor [3,16,17,20,21,43].

NFs undergo a reduction in transport velocity during development and following maturation [10,11,42]. The rate

of NF axonal transport is subject to multiple variables, including alterations in subunit synthesis, incorporation into Triton-insoluble structures, and C-terminal phosphorylation. General factors that also can contribute to NF transport velocity include changes in overall axonal transport and axonal caliber, as well as non-specified age-related effects, such as an overall decline in metabolism. In the present study, we probed the influence of NF C-terminal phosphorylation on axonal transport by using a brief window of time in young adult mice that excludes or minimizes the potential contribution of the above other factors.

2. Materials and methods

2.1. Injection of radiolabel and harvesting of tissues

Murine retinal ganglion cells were radiolabeled in situ by injection of 70 μ Ci ³⁵S-methionine in a total volume of

* Corresponding author. Fax: +1-508-934-3044; e-mail: thomas_shea@uml.edu

0.2 μ l via a pulled glass capillary pipette into the vitreous of anesthetized mice of either 2 months or 5 months of age as described [13,36]. Mice were sacrificed by cervical dislocation at intervals of 6 h–60 days following injection. Retinas were dissected away from the rest of the eye and optic axons dissected into 9×1.1 mm segments on a glass slide on dry ice. Retinas and axonal segments from both eyes of 5 mice were pooled and homogenized in 1% Triton X-100 in 50 mM Tris (pH 6.9) containing 2 mM EDTA, 1 mM PMSF and 50 μ g/ml leupeptin at 4°C by 50 strokes in a tight-fitting glass-Teflon homogenizer; 11 mice were used for samples to be harvested at 60 days after injection. The Triton-insoluble cytoskeleton was sedimented by centrifugation $15,000 \times g$ for 15 min as described [4].

2.2. Gel electrophoresis, autoradiography and immunoblot analyses

NF subunits were immunoprecipitated from cytoskeletons by standard methods using a polyclonal antibody (R39; diluted 1:150) that immunoprecipitates all 3 NF subunits followed by protein A-sepharose (Sigma) as described [32,36]. Immunoprecipitated material was subjected to SDS-gel electrophoresis on linear 7% acrylamide gels. This antibody also immunoprecipitates fodrin and high molecular-weight MAPs [13,36]. Electrophoretically separated proteins were transferred to nitrocellulose or gels were Coomassie-stained, photographed, and dried for generation of autoradiographs. Immunoblots were generated as described previously [36]. Pre-immune sera, or commercially obtained non-immune sera, did not react with any NF-related polypeptides, and omission of primary antibodies in immunoblot analysis failed to generate reactive species.

2.3. Densitometric analyses and calculation of transport rates

Autoradiographs and nitrocellulose replicas were digitized via a UMax scanner equipped with a transparency adaptor operated by a Macintosh Power PC. Densitometric analyses of digitized images were carried out via NIH Image software by encircling the entire band with the program's freehand selection tool as described previously [5]. Total mean density, following two-dimensional automated background subtraction, was calculated for autoradiographs and immunoblots. Manual subtraction of background for individual bands yielded identical values as automated subtraction. Repeated scanning of samples yielded no appreciable variance in net densitometric values. Since the NF triplet co-migrated along optic axons, densitometric data are presented only for NF-L for simplicity only [13,17].

The transport rate of NF subunits was determined for location of the peak and front of total subunit radioactivity using previously established methods [2,10,42]. The location of the peak was determined by graphic representation of relative densities of each segment (densitometric units vs. distance in mm), followed by constructing a vertical line which bisected 2/3 of the maximum height of the curve and determining the intersection of this line with the x axis as described previously [10]. The location of the front of subunit transport was determined using these same curves by the intersection of a line tangential to the leading slope with the x axis [42]. Transport rates in mm/day were then determined as the distance migrated (mm) at a given interval divided by the number of days in that interval. Raw densitometric values, expressed in arbitrary units and presented as the mean \pm S.D. are also expressed as the fold increase obtained at 5 months vs. that obtained for 2 months (obtained by dividing individual values for segments 1–9 of 5-month-old mice by those obtained for 2-month-old mice). The relative increase in R39 and RT97 immunoreactivity along axons was obtained by dividing densitometric values obtained for each segment by that obtained for segment 1. Finally, the relative increase in RT97 vs. R39 immunoreactivity along axons was calculated by dividing (segment by segment) the relative increase between 2 and 5 months for RT97 by that obtained for R39. All gels, autoradiographs and immunoblots were generated from pools of 5 mice per sample in each experiment (except for 60 days of chase, which utilized 11 mice; above). Both eyes were injected, and both pathways harvested and pooled for all mice. Multiple autoradiographs of differing exposures were generated to insure linearity, and all scanning and densitometric operations were carried out within a linear range that included all pixels within a selected band, yet did not allow saturation of any pixels, and excluded all pixels within adjacent background areas.

3. Results

Immunoblot analyses of optic axons with an antibody (R39) that recognizes all NF subunits (Fig. 1), and analyses of Coomassie-stained gels of immunoprecipitated NF subunits (Fig. 2) demonstrated an increase in NFs along the length of murine optic axons at both 2 and 5 months of age. This increase was paralleled by an increase in phosphorylated (200 kDa) NF-H as revealed both by Coomassie-staining and by R39 immunoreactivity (Figs. 1 and 2), indicating that the proximal–distal increase in total NFs was accompanied by an increase in phospho-NFs. Total NF levels and distribution, as ascertained by Coomassie staining of NF-L in immunoprecipitates did not change appreciably between 2 and 5 months of age (Fig. 2). These findings are in agreement with the previous ultrastructural demonstration that the full complement of

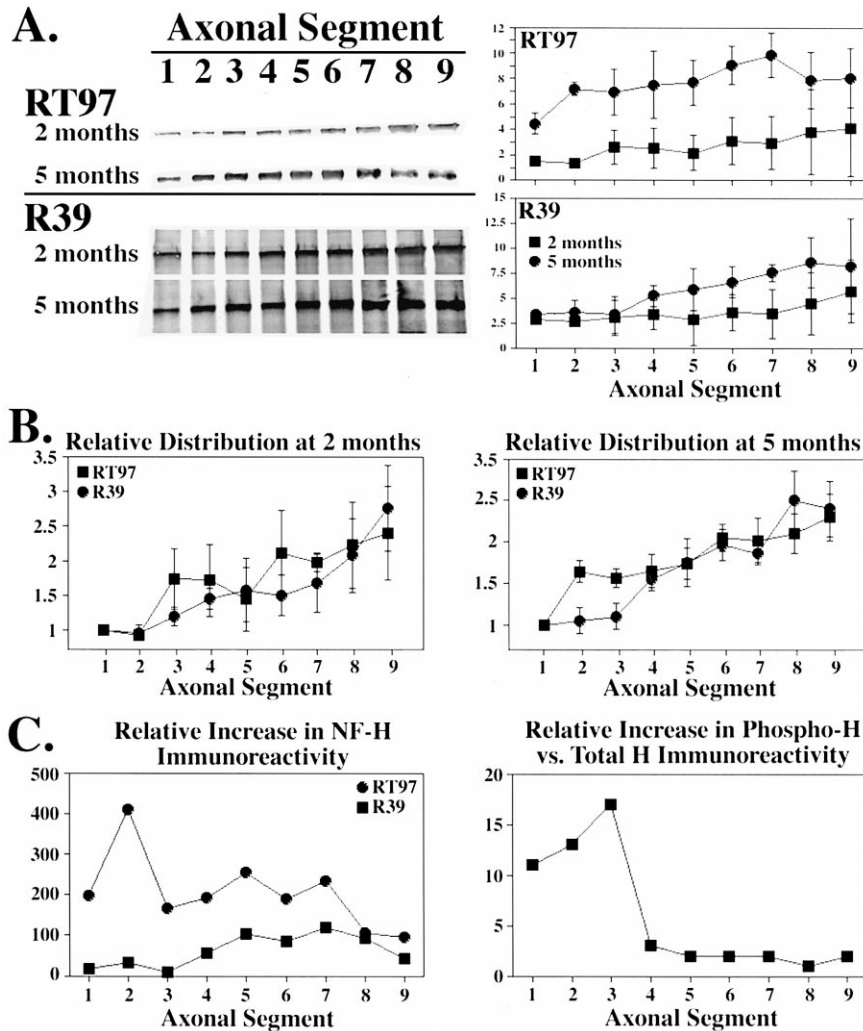


Fig. 1. NFs undergo an increase in C-terminal phosphorylation between 2 and 5 months of age. Panel A: Nitrocellulose replicas were immunostained with R39, which visualizes all NFs regardless of phosphorylation state, and RT97, which recognizes a developmentally delayed NF-H C-terminal phospho-epitope; only the 200-kDa region is presented. The accompanying graphs present the distribution (expressed in arbitrary densitometric units) of RT97- and R39-immunoreactive NF in optic axonal cytoskeletons at 2 and 5 months of age. Total 200 kDa NF-H undergoes a modest increase by 5 months of age, while RT97-immunoreactive NF-H undergoes a much larger increase. Panel B: Graphs compare the relative distribution of R39 and, separately, RT97 at 2 and 5 months of age. Values were obtained by dividing the above arbitrary densitometric units obtained for each segment by the value obtained for segment 1. Calculations were carried out separately for each experimental determination, and the data were then pooled to obtain mean and standard deviations for each time point. Note the significant increase in RT97 immunoreactivity within the proximal region of axons. Panel C: Comparison of the relative increases in R39 and RT97 immunoreactivity between 2 and 5 months (calculated by dividing densitometric values obtained for pools of segments at 5 months by those obtained at 2 months), and the relative increase in RT97 immunoreactivity vs. R39 immunoreactivity (calculated by dividing the above ratio for RT97 by that obtained for R39). Presentation in this manner highlights that, while both R39 and RT97 immunoreactivity increase between 2 and 5 months, a pronounced increase in RT97 immunoreactivity occurs within proximal axons.

adult NFs are present by 2 months of age, and that NFs undergo a proximo-distal increase [22,25]. However, an increase in 200 kDa NF-H was detected between 2 and 5 months of age as visualized by immunoreactivity with the polyclonal, phospho-independent anti-NF antibody R39 (Figs. 1 and 2). An even more marked increase in immunoreactivity with an antibody (RT97) directed against a developmentally-delayed NF-H C-terminal phospho-epitope [1] was observed between 2 and 5 months of age (Fig. 1). NF-H bearing the RT97 epitope demonstrated an ap-

proximately 3-fold increase in RT97 immunoreactivity with segment 1, 5-fold within segment 2, and approximately 2-fold increases in segments 3-7 (Fig. 1). These data indicate that NFs underwent significantly more C-terminal phosphorylation by 5 months of age vs. that present at 2 months of age. Comparison of the relative increases in RT97 and R39 immunoreactivity demonstrated that the most pronounced developmental increase was observed within the most proximal axonal region (i.e., the first few axonal segments; Fig. 1).

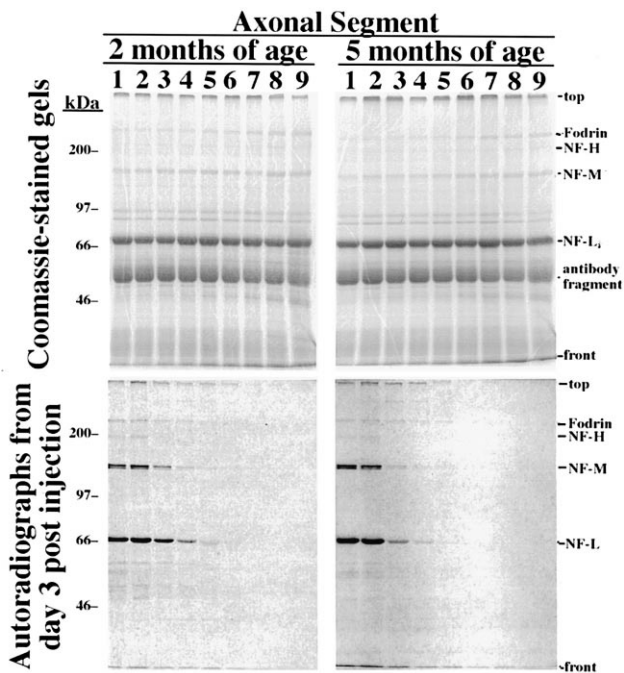


Fig. 2. Immunoprecipitation of NFs and autoradiographic analysis of NF axonal transport. Panels present Coomassie blue-stained gels and resultant autoradiographs of material immunoprecipitated by R39 from cytoskeletons of axonal segments of 2- and 5-month-old mice that were intravitreally injected with ³⁵S-methionine radiolabel 3 days previously. The migratory positions of fodrin, 200 kDa NF-H, 145 kDa NF-M, 70 kDa NF-L and (in Coomassie-stained gels) antibody fragments derived from immunoprecipitation are indicated. Note the similar levels of NFs at 2 and 5 months of age.

We next examined whether differences were observed in NF axonal transport between 2 and 5 months of age. NF axonal transport was monitored at intervals by autoradiographic analyses following intravitreal injection of ³⁵S-methionine radiolabel and immunoprecipitation of NF subunits. Consistent with previous studies [13,16,17,22,36,42], transport of NF subunits into optic axons initiated within hours after injection of radiolabel into both 2- and 5-month-old mice, and the profile of radiolabeled subunits broadened during continued transport at each age (Fig. 2). NF transport rates were monitored by following the location of the peak and the front of the wave of radiolabeled NF-L as described previously [2,10]. Both the peak and the front of radiolabeled NF-L advanced more rapidly in 2 month-old mice vs. 5-month-old mice as revealed both by visual inspection (Fig. 3) and by densitometric analyses of autoradiographs (Fig. 4). At day 6 after injection, for example, the front of radiolabeled NF subunits in 5-month-old mice had traveled only into segment 7, while that of 2-month-old mice had reached segment 9 (Fig. 4). Although groups of mice were harvested and NFs subjected to radiography at 60 days following injection, this time point was not included in densitometric analyses, since visual inspection of autoradiographs demonstrated that the

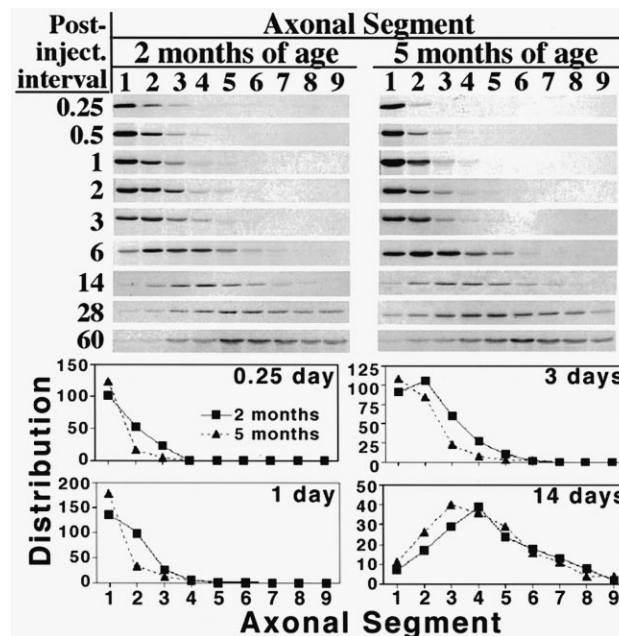


Fig. 3. Distribution of radiolabeled NF subunits along optic axons. Panels present autoradiographic analyses of the distribution of radiolabeled NF-L along optic axons from 2- and 5-month-old mice harvested at intervals following intravitreal injection of radiolabel as indicated. The accompanying graphs present densitometric analysis of the distribution of radiolabeled NF-L from 2- and 5-month-old mice harvested at the indicated intervals following labeling; values for each segment are expressed as a percent of the total radiolabeled subunits at each sampling interval. As shown previously, newly-synthesized NF subunits enter axons within hours and undergo continued transport along axons. Visual inspection of autoradiographs, as well as densitometric analyses, reveals that NF subunits undergo more rapid transport in optic axons from 2-month-old mice as compared to 5-month-old mice.

peak of radiolabeled subunits had reached the axon terminals before this time (Fig. 3).

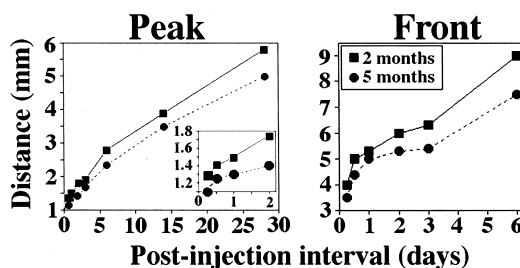


Fig. 4. Analysis of NF transport in optic axons. Graphs present the migration of the peak and front of the wave of radiolabeled NF-L in optic axons from 2- and 5-month-old mice, expressed as the distance migrated vs. post-injection interval calculated according to previous studies as described in Section 2. The inset in the graph of the peak distribution more clearly presents days 1 and 2 following radiolabeling. Data for the peak is presented up to day 28 only, since by day 60 (the next time point examined), the peak had traversed the axonal length. Similarly, data for the front is presented only up to day 6, since 2-month-old mice had reached the terminal axonal segment by this time. Comparison of migration of both the peak and the front of the wave of radiolabeled NFs reveals that NFs are transported more rapidly in 2- vs. 5-month-old mice.

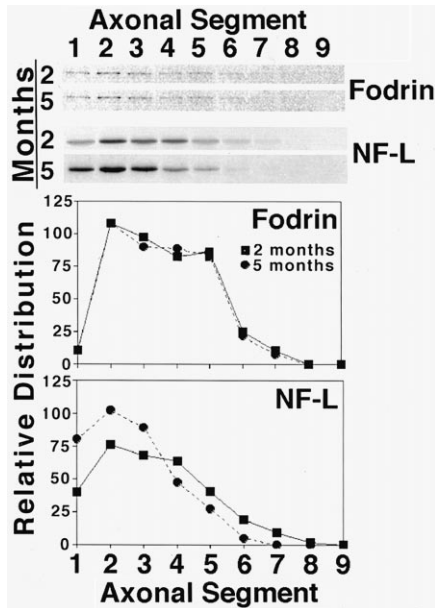


Fig. 5. Axonal transport of fodrin does not decline between 2 and 5 months of age. Panels present autoradiographic analyses of fodrin and NFs immunoprecipitated from optic axons of 2- and 5-month-old mice 6 days after injection of radiolabel. The accompanying graphs present densitometric analyses of the distribution of these proteins expressed in arbitrary densitometric units. Note that the relative distribution of fodrin does not vary appreciably between 2 and 5 months of age, while that of NF-L (derived from the identical samples) undergoes a significant slowing in transport. The identity of fodrin was confirmed by immunoblot analyses with an anti-fodrin antibody (not shown; see Refs. [13,40]).

These differential NF transport rates were not artifactually generated by any difference in incorporation of NFs into the cytoskeleton, as no difference was observed in total radiolabeled NFs recovered within cytoskeletons along

the entire axonal length during these analyses: total densitometric values of newly synthesized NFs was 276 ± 60 (mean \pm S.E. of the mean; arbitrary densitometric units) for mice at 2 months of age and 271 ± 36 for mice at 5 months of age ($p < 0.94$; Student's *t*-test, values calculated using 8 groups of 5–11 mice for each age). The slowing observed for NF transport between 2 and 5 months of age was not a reflection of an overall decline in slow axonal transport, since fodrin exhibited an apparently identical transport rate at 2 and 5 months of age (Fig. 5).

Comparison of relative transport rates at within each sampling interval (calculated by dividing the distance which the peak has traveled during that interval by the number of days in that interval; Table 1) demonstrated that, as expected, NF subunits in both 2-month-old and 5-month-old pools of mice underwent progressive proximal–distal slowing in transport rates along their respective axonal lengths [10,11,42]. While the front of the radiolabeled NF wave undergoes overall transport more rapidly than does the peak [17], a similar situation was observed for the front of the wave at 2 vs. 5 months of transport (Table 1). In addition, however, we noted that the transport rate of the peak in 5-month-old mice maintained an average rate of approximately 85% that of 2-month-old mice for the entire axonal length (Table 1). That is, transport of NFs in 5-month-old mice at the first day examined, and within the first segment of optic axons, was approximately 85% that of 2-month-old mice, with no further decline in relative transport rate between 2- and 5-month-old mice along the entire axonal length. Similarly, the front of the wave transported at an average of approximately 88% slower in 5-month-old vs. 2-month-old mice; this developmental reduction was apparent in the first segment, and remained essentially the same relative rate, for the entire axonal length (Table 1).

Table 1

Comparative distance traveled and axonal transport rates of 2- and 5-month-old mice

The migratory distance of the peak and front at each time point was derived as described previously (see Section 2). Rates presented for each interval were calculated by dividing the distance traveled within a given interval by the number of days in that interval. Comparative rates of 5-month-old vs. 2-month-old mice were obtained by dividing rates for each interval at 5 months/rates at 2 months \times 100. Values are presented up to day 28 for the peak and day 6 for the front, since by the next respective time point examined in each case, the peak and front had exited the axon

Time post injection	Peak values*					Front values**				
	Distance (mm)		Rate (mm/day)		Rate, 5 vs. 2 months (%)	Distance (mm)		Rate (mm/day)		Rate, 5 vs. 2 months (%)
	2 months	5 months	2 months	5 months		2 months	5 months	2 months	5 months	
0.25	1.3	1.1	5.20	4.40	85	4	3.5	16	14	88
0.5	1.4	1.25	2.80	2.50	89	5	4.4	10	8.8	88
1	1.5	1.3	1.50	1.30	87	5.3	5	5.3	5	94
2	1.75	1.4	0.88	0.70	80	6	5.3	6	5.3	88
3	1.9	1.7	0.63	0.57	89	6.3	5.4	3.15	2.7	86
6	2.8	2.35	0.47	0.39	84	9	7.5	3	2.5	83
14	3.9	3.5	0.28	0.25	90					
28	5.8	5	0.21	0.18	86					

4. Discussion

We describe herein a developmental decrease in NF axonal transport within optic axons that is correlated with an increase in a developmentally delayed, NF-H C-terminal phospho-epitope. This modest decrease observed herein would certainly be greater had we utilized a larger range of mouse ages. However, we purposely selected a short developmental window in order to isolate as best as possible NF C-term phosphorylation as a potential regulatory influence on NF transport. In this regard, we were unable to initiate these studies prior to the appearance of RT97, since this epitope is prominent as early as 1 month of post-natal development (not shown), yet optic axons have not completed their caliber increase before at least 1 month [30]. Instead, we initiated our studies at 2 months of age, well after the time at which optic axons had already attained adult proportions, and chose a relatively close final point (5 months) in efforts to preclude overall age-related effects that may contribute to a reduction in transport velocity. As described previously for mature peripheral nerves [42], NFs in these mature optic axons underwent a progressive slowing of transport velocity along the length of axons. This proximal–distal slowing was identical in both ages examined, but was accompanied by an additional overall decline in NF transport rate between 2 and 5 months of age. The extent of this decline (approximately 15%) was relatively modest in comparison to the developmental declines observed in peripheral nerve [10,11]. However, even during peripheral nerve development, the most dramatic developmental decline occurred during the earlier stages examined (e.g., 3–10 weeks of age), with a 6-fold decrease in the rate of decline during occurring during the later stages examined (10–20 weeks), despite an ongoing linear increase in axonal caliber [10]. This latter observation indicates that caliber increase alone cannot account fully for the developmental decline in NF transport [42]. Observation of progressive slowing of NF axonal transport in mature axons indeed eliminates the contribution of certain developmental effects; however, in these latter studies, the potential effects of phosphorylation were not directly measured [42].

The major factors which may influence NF axonal transport include: (1) NF synthesis and incorporation into the axonal cytoskeleton [11], (2) overall axonal transport rates [11], (3) increases in axonal caliber [10,11], (4) overall axonal NF levels [25], and (5) NF C-terminal phosphorylation [2,19,25,42]. The results of this study eliminate most of these possibilities as follows: (1) No change was observed in levels of NFs incorporating into the cytoskeleton; (2) no decline in overall slow axonal transport has occurred between 2 and 5 months of age, since fodrin did not undergo a decline in transport rate during this interval; (3) murine optic axons have undergone caliber expansion by 30 days of post-natal development [30]; and, finally, (4) direct quantification of NFs in

ultrastructural analyses has reported that no increase in NFs occurs beyond 2 months of age [30], which was corroborated herein by electrophoretic analyses of total NF protein. However, a major developmental increase in C-terminal NF-H phosphorylation, reflected by RT97 immunoreactivity, did occur between 2 and 5 months of age. These findings collectively support the notion that C-terminal NF-H phosphorylation regulates axonal transport.

Comparison of the initial rate of NF transport (i.e., within the first day) demonstrated that NF subunits in 5-month-old mice already exhibited a transport rate approximately 85% of that of 2-month-old mice. Calculation of transport rates along the axonal length in mm/day for each time interval examined further revealed that 2- and 5-month-old mice essentially maintained that same relative rates; that is, 5-month-old mice continued to undergo transport at an average rate of 85% of that of 2-month-old mice along the entire axonal length. These calculations suggest that the factors influencing the difference in transport rate between 2- and 5-month-old mice are encountered within the retina or within the most proximal region of optic axons. While C-terminal NF phosphorylation initiates within retinal ganglion neuronal perikarya [36], the proximal region of optic axons has previously been noted as the region in which NFs undergo a dramatic increase in site-specific C-terminal NF-H phosphorylation, which is reflected by an increase in the RT97 epitope [25]. This regional increase in C-terminal phosphorylation has been considered to play an important role in decreasing local NF transport [25]. Comparative immunoblot analyses demonstrated that, during the time period examined herein, RT97 underwent its most profound increase within the proximal region of optic axons. One interpretation of the findings of this study is that one or more C-terminal NF phosphorylation events, which correlate with increased RT97 immunoreactivity, have a negative impact on NF axonal transport velocity. In support of this conclusion, inhibition of phosphatase activities within optic axons increases RT97 immunoreactivity within retina and proximal axons and slows transport [14]. Moreover, in recent studies demonstrating that kinesin participates in NF transport in optic axons, RT97-immunoreactive NFs were selectively not associated with kinesin, suggesting that site-specific C-terminal phosphorylation events may dissociate NFs from their putative transport motor [43].

While increased NF phosphorylation in some studies was correlated with decreased slow axonal transport [8,9,25], it was correlated with increased transport in others [6,41]. These divergent results prompted the suggestion that the relationship between NF phosphorylation and axonal transport is likely to be complex, such that some phosphorylation event(s) may foster association between NFs [7,18,19,25,34,35], while other event(s) may regulate the coupling of NFs with the transport motor [6]. However, a role for NF-H phosphorylation in dissociation from a motor complex and/or increased NF-NF association is

consistent with the recent demonstration that NF transport velocity is slightly but significantly faster in mice lacking NF-H [45].

Acknowledgements

This research was supported by National Science Foundation grant IBN-9809878. The technical assistance of Daniela Ortiz is acknowledged.

References

- [1] B.H. Anderton, D. Breinburg, M.J. Downes, P.J. Green, B.E. Tomlinson, J. Ulrich, J.N. Wood, J. Kahn, Monoclonal antibodies show that neurofibrillary tangles and neurofilaments share antigenic determinants, *Nature* 298 (1982) 84–86.
- [2] D.R. Archer, D.F. Watson, J.W. Griffin, Phosphorylation-dependent immunoreactivity of neurofilaments and the rate of slow axonal transport in the central and peripheral axons of the rat dorsal root ganglion, *J. Neurochem.* 62 (1994) 1119–1125.
- [3] P.W. Baas, A. Brown, Slow axonal transport: The polymer transport model, *Trends Cell Biol.* 7 (1997) 380–384.
- [4] F.-C. Chiu, W.T. Norton, Bulk preparation of CNS cytoskeleton and the separation of individual neurofilament proteins by gel filtration: dye-binding characteristics and amino acid compositions, *J. Neurochem.* 39 (1982) 1252–1260.
- [5] C.M. Cressman, T.B. Shea, Hyperphosphorylation of Tau and filopodial retraction following microinjection of protein kinase C catalytic subunits, *J. Neurosci. Res.* 42 (1995) 648–656.
- [6] S.M. deWaegh, V.M.-Y. Lee, S.T. Brady, Local modulation of neurofilament phosphorylation, axonal caliber, and slow axonal transport by myelinating Schwann cells, *Cell* 68 (1992) 451–463.
- [7] J. Eyer, J.F. Leterrier, Influence of the phosphorylation state of neurofilament proteins on the interactions between purified filaments in vitro, *Biochem. J.* 252 (1988) 655–660.
- [8] J.W. Griffin, D.L. Price, P.N. Hoffman, Neurotoxic probes of the axonal cytoskeleton, *Trends Neurosci.* 6 (1983) 490–495.
- [9] J.W. Griffin, D.F. Watson, Axonal transport in neurological disease, *Ann. Neurol.* 23 (1988) 3–13.
- [10] P.N. Hoffman, R.J. Lasek, J.W. Griffin, D.L. Price, Slowing of the axonal transport of neurofilament protein during development, *J. Neurosci.* 3 (1983) 1694–1700.
- [11] P.N. Hoffman, J.W. Griffin, B.G. Gold, D.L. Price, Slowing of neurofilament transport and the radial growth of developing nerve fibers, *J. Neurosci.* 5 (1985) 2920–2929.
- [12] C. Jung, J.T. Yabe, F.-S. Wang, T.B. Shea, Neurofilaments undergo translocation into axonal neurites before incorporation into Triton-insoluble structures, *Cell Motil. Cytoskeleton* 40 (1998) 44–58.
- [13] C. Jung, T.B. Shea, Regional decline in NF axonal transport: correlation with NF-H phosphorylation, *Mol. Biol. Cell* 8 (1997) 279a.
- [14] Y. Komiya, T. Tashiro, M. Kuokawa, Phosphorylation of neurofilament proteins during their axonal transport, *Biomed. Res.* 7 (1986) 345–348.
- [15] R.J. Lasek, P. Paggi, M.J. Katz, Slow axonal transport mechanisms move neurofilaments relentlessly in mouse optic axons, *J. Cell Biol.* 117 (1992) 607–616.
- [16] R.J. Lasek, P. Paggi, M.J. Katz, The maximum rate of neurofilament transport in axons: A view of molecular transport mechanisms continuously engaged, *Brain Res.* 616 (1993) 58–64.
- [17] J.F. Leterrier, Eyer, Properties of highly viscous gels formed by neurofilaments in vitro. A possible consequence of a specific inter-filament cross-bridging, *Biochem. J.* 245 (1987) 93–101.
- [18] S.E. Lewis, R.A. Nixon, Multiple phosphorylated variants of the high molecular mass subunit of neurofilaments in axons of retinal cell neurons: Characterization and evidence for their differential association with stationary and moving neurofilaments, *J. Cell Biol.* 107 (1988) 2689–2701.
- [19] R.A. Nixon, The regulation of neurofilament protein dynamics by phosphorylation: clues to neurofibrillary pathobiology, *Brain Pathol.* 3 (1993) 29–38.
- [20] R.A. Nixon, The slow axonal transport of cytoskeletal proteins, *Curr. Opin. Cell Biol.* 10 (1988) 87–92.
- [21] R.A. Nixon, K.B. Logvinenko, Multiple fates of newly synthesized neurofilament proteins: Evidence for a stationary neurofilament network distributed non-uniformly along axons of retinal ganglion cell neurons, *J. Cell Biol.* 102 (1986) 647–659.
- [22] R.A. Nixon, S.E. Lewis, M. Mercken, R.K. Sihag, ³²P-orthophosphate and ³⁵S-methionine label separate pools of neurofilaments with markedly different axonal transport kinetics in mouse retinal ganglion cells in vivo, *Neurochem. Res.* 19 (1994) 1445–1453.
- [23] R.A. Nixon, P.A. Paskevich, R.A. Sihag, C.Y. Thayer, Phosphorylation on carboxyl terminus domains of neurofilament proteins in retinal ganglion cell neurons in vivo: influences on regional neurofilament accumulation, interneurofilament spacing, and axon caliber, *J. Cell Biol.* 126 (1994) 1031–1046.
- [24] S. Okabe, N. Hirokawa, Dynamics of neuronal intermediate filaments, *Mol. Biol. Cell* 3 (1992) 355, abstr.
- [25] H.C. Pant, T. Yoshioka, I. Tasaki, Divalent cation dependent phosphorylation of proteins in squid giant axon, *Brain Res.* 162 (1979) 303–313.
- [26] M.S. Runge, M.R. El-Maghrabi, T.H. Claus, S.J. Pilgis, R.C. Williams, A MAP-2 stimulated protein kinase activity associated with neurofilaments, *Biochemistry* 20 (1981) 175–180.
- [27] I. Sanchez, L. Hassinger, P.A. Paskevich, H.D. Shine, R.A. Nixon, Oligodendroglial regulate the regional expansion of axon caliber and local accumulation of neurofilaments during development independently of myelin formation, *J. Neurosci.* 16 (1996) 5095–5105.
- [28] G. Schekert, R.J. Lasek, Neurofilament protein phosphorylation, *J. Biol. Chem.* 257 (1982) 4788–4795.
- [29] T.B. Shea, R.K. Sihag, R.A. Nixon, Dynamics of phosphorylation and assembly of the high molecular weight neurofilament protein subunit in NB2a/d1 neuroblastoma, *J. Neurochem.* 55 (1990) 1784–1792.
- [30] T.B. Shea, P.A. Paskevich, M.L. Beermann, The protein phosphatase inhibitor okadaic acid increases axonal neurofilaments and neurite caliber, and decreases axonal microtubules in NB2a/d1 cells, *J. Neurosci. Res.* 35 (1992) 507–521.
- [31] T.B. Shea, M.L. Beermann, Respective roles of neurofilaments, microtubules, MAP1b and tau in neurite outgrowth and stabilization, *Mol. Biol. Cell* 5 (1994) 863–875.
- [32] T.B. Shea, M.L. Beermann, Multiple interactions of aluminum with neurofilament subunits: regulation by phosphate-dependent interactions between C-terminal extensions of the high and middle molecular weight subunits, *J. Neurosci. Res.* 38 (1994) 160–166.
- [33] T.B. Shea, D. Dahl, R.A. Nixon, I. Fischer, Triton-soluble phospho-variants of the heavy neurofilament subunit in developing and mature mouse central nervous system, *J. Neurosci. Res.* 48 (1997) 515–523.
- [34] R.K. Sihag, R.A. Nixon, In vivo phosphorylation of distinct domains of the 70-kilodalton neurofilament subunit involves different protein kinases, *J. Biol. Chem.* 264 (1989) 457–464.
- [35] R.K. Sihag, R.A. Nixon, Phosphorylation of the amino-terminal head domain of the middle molecular mass 145 kDa subunit of neurofilaments: Evidence for regulation by second messenger-dependent protein kinases, *J. Biol. Chem.* 265 (1990) 4166–4171.
- [36] R.K. Sihag, R.A. Nixon, Identification of Ser-55 as a major protein kinase A phosphorylation site on the 70-kDa subunit of neurofila-

- ments: Early turnover during axonal transport, *J. Biol. Chem.* 266 (1991) 18861–18867.
- [40] R.K. Sihag, T.B. Shea, F.-S. Wang, Spectrin-actin interaction is required for neurite extension in NB2a/d1 neuroblastoma cells, *J. Neurosci. Res.* 44 (1996) 430–437.
- [41] M. Tsuda, T. Tashiro, Y. Komiya, Increased solubility of high-molecular mass neurofilament subunit by suppression of dephosphorylation: its relation to axonal transport, *J. Neurochem.* 68 (1997) 2558–2565.
- [42] D.F. Watson, P.N. Hoffman, K.P. Fittro, J.W. Griffin, Neurofilament and tubulin transport slows along the course of mature motor axons, *Brain Res.* 477 (1989) 225–232.
- [43] J. Yabe, C. Jung, T.B. Shea, Regulation of neurofilament axonal transport by phosphorylation in optic axons in situ: involvement of the microtubule motor protein kinesin, *Mol. Biol. Cell* 9 (1998) in press.
- [44] B. Zhang, P. Tu, F. Abtahian, J.Q. Trojanowski, V.M.-Y. Lee, Neurofilaments and orthograde transport are reduced in ventral root axons of transgenic mice that express human SOD1 with a G93A mutation, *J. Cell Biol.* 139 (1997) 1307–1315.
- [45] Q. Zhu, M. Lindenbaum, E. Levavassuer, H. Jacomy, J.-P. Julien, Disruption of the NF-H gene increases axonal microtubule content and velocity of neurofilament transport: relief of axonopathy resulting from the toxin β,β -iminopropionitrile, *J. Cell Biol.* 143 (1998) 183–193.